ELectronics EXpress

IEICE Electronics Express, Vol.1, No.11, 298–304

Raman induced wavelength conversion in scaled Silicon waveguides

Varun Raghunathan, Dimitris Dimitropoulos, Ricardo Claps, and Bahram Jalali[a)]

Electrical Engineering department, University of California Los Angeles

420 Westwood Plaza, Los Angeles, CA: 90095, USA

a) *jalali@ucla.edu*

Abstract: Parametric Raman nonlinearities in Silicon waveguides is used to demonstrate wavelength conversion from Stokes to anti-Stokes channels. The effects of two photon absorption and free carrier nonlinear losses on the conversion process have also been analyzed. We find that scaling down the waveguide dimensions to submicron sizes is advantageous in terms of increasing the Raman nonlinearities and reducing the carrier lifetime and hence nonlinear absorption.

Keywords: Integrated optics, Nonlinear optics, Raman scattering, Wavelength conversion

Classification: Photonics devices, circuits, and systems

References

[1] G. T. Reed, "Optical age of Silicon," *Nature*, vol. 427, pp. 595–596, 2004.

[2] S. J. B. Yoo, "Wavelength conversion technologies for WDM network applications," *J. Lightwave Technol.*, vol. 14, pp. 955–966, 1996.

[3] R. Claps, D. Dimitropoulos, V. Raghunathan, and B. Jalali, "Observation of Stimulated Raman amplification in Silicon waveguides," *Opt. Express*, vol. 11, pp. 1731–1739, 2003.

[4] A. Villeneuve et al., "Nonlinear Absorption in a GaAs Waveguide Just Above Half the Band Gap," *IEEE J. Quantum Electron.*, vol. 30, pp. 1172–1175, 1994.

[5] T. K. Liang and H. K. Tsang, "Role of free carriers from two-photon absorption in Raman amplification in silicon-on-insulator waveguides," *Appl. Phys. Lett.*, vol. 84, pp. 2745–2747, 2004.

[6] R. A. Soref and B. R. Bennett, "Electrooptical Effects in Silicon," *IEEE J. Quantum Electron.*, vol. 23, pp. 123–129, 1987.

[7] R. Claps, V. Raghunathan, D. Dimitropoulos, and B. Jalali, "Influence of non-linear absorption on Raman amplification in Silicon waveguides," *Opt. Express*, vol. 20, pp. 2774–2780, 2004.

[8] E. Golovchenko, P. V. Mamyshev, A. N. Pilipetskii, and E. M. Dianov, "Mutual Influence of the Parametric Effects and Stimulated Raman Scattering in Optical Fibers," *IEEE J. Quantum Electron.*, vol. 26, pp. 1815–1820, 1990.

[9] D. Dimitropoulos, V. Raghunathan, R. Claps, and B. Jalali, "Phase-matching and Nonlinear Optical Processes in Silicon Waveguides," *Opt. Express*, vol. 12, pp. 149–160, 2004.

DOI: 10.1587/elex.1.298
Received August 03, 2004
Accepted August 05, 2004
Published September 10, 2004

[10] R. Claps, V. Raghunathan, D. Dimitropoulos, and B. Jalali, "Anti-Stokes Raman conversion in Silicon waveguides," *Opt. Express*, vol. 11, pp. 2862–2872, 2003.
[11] V. Raghunathan, R. Claps, D. Dimitropoulos, and B. Jalali, "Wavelength conversion in Silicon using Raman induced four-wave mixing," *Appl. Phys. Lett.*, vol. 84, pp. 34–36, 2004.
[12] R. J. Bozeat et al., "Silicon Based Waveguides," Silicon Photonics. Eds, Pavesi, L., Lockwood, D. J. Springer-Verlag. ch. 8, pp. 269–294, 2004.
[13] L. Tong et al., "Single-mode guiding properties of subwavelength diameter silica and silicon wire waveguides," *Opt. Express*, vol. 12, pp. 1025–1035, 2004.

1 Introduction

The success of silicon as the mainstay of the electronic industry has fuelled interest in using the technology to create low-cost optical and opto-electronic integrated circuits. Research on silicon photonics was started in the 1980's with significant progress, accelerated by the telecommunication boom, during the late 1990's. Despite success in making high quality wavelength filters and other passive devices, silicon photonics has been hindered by the lack of suitable active functionality. Recently good progress has been made toward light generation and amplification, modulation, and detection using silicon [1]. Wavelength conversion is another fundamental function required in multi-wavelength optical communications. In this paper, we discuss parametric Raman interactions in silicon, and report the observation of wavelength conversion in waveguides with submicron modal area. We find that scaling down the waveguide dimensions to submicron sizes is advantageous in terms of increasing the Raman nonlinearities and reducing the carrier lifetime and hence nonlinear absorption. Such nanoscale waveguides also offer flexibility in achieving phase matching.

2 Theory

Conventionally, wavelength conversion is performed in optical fibers by making use of the broadband electronic susceptibility, $\chi_E^{(3)}$ of the material [2]. In contrast, the technique described here makes use of the resonant Raman-induced optical susceptibility, with a peak ($\chi_R^{(3)} = 11.2 \times 10^{-14}\, cm^2/V^2$) that is ∼44 times stronger than the electronic susceptibility in silicon ($\chi_E^{(3)} = 0.25 \times 10^{-14}\, cm^2/V^2$). The vibrational energy levels of Silicon and the Raman induced wavelength conversion process are shown in Fig. 1 (a). When the pump, Stokes, and anti-Stokes fields are phase matched ($\Delta k = 2k_P\text{-}k_S\text{-}k_A = 0$), the two processes shown in Fig. 1 (a) couple through the mediation of coherent phonons and this leads to coherent transfer of information between the Stokes and anti-Stokes channels.

Another non-linear process that could compete with Raman scattering is Two-Photon absorption (TPA). At power levels achievable under continuous wave pumping, depletion of the pump due to TPA is negligible [3]. However,

DOI: 10.1587/elex.1.298
Received August 03, 2004
Accepted August 05, 2004
Published September 10, 2004

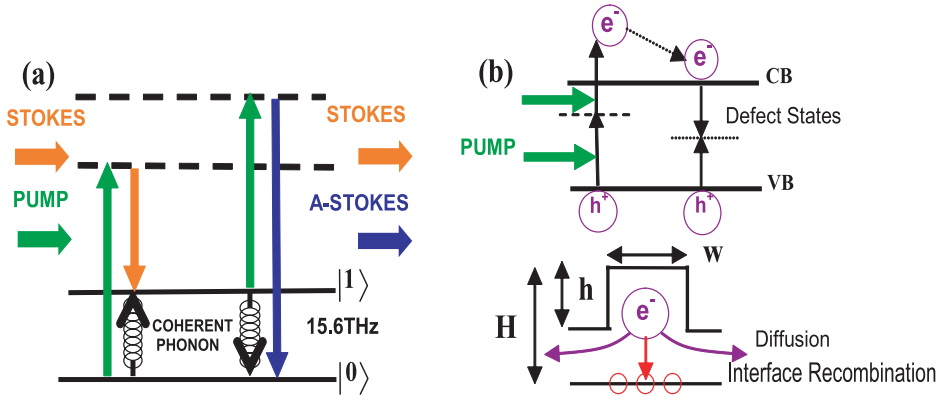

Fig. 1. (a) The vibrational energy levels of Silicon showing the Raman wavelength conversion process. (b) Electronic energy levels of Silicon and Two-photon absorption (TPA) process. Free carriers generated by TPA increase the overall loss. These free carriers diffuse out of the rib structure and also recombine at interface defect states. In this work, w = 2 μm, H = 0.93 μm and h = 0.45 μm.

the free-carriers generated during this process increase waveguide losses and lower the conversion efficiency through free carrier absorption. The electronic energy levels of Silicon and TPA induced free carrier generation are shown in Fig. 1 (b). This has been identified as a limitation in all-optical switching in III-V semiconductor waveguides [4] and has also been observed in silicon waveguides [5]. The TPA-induced free carrier loss is described by the Drude model as [6]: $\Delta\alpha_{FCA} \cong 6.04 \times 10^{-18}\lambda^2(\mu m) \cdot \beta I_p^2 \tau_{eff}/2E_p$. Here, β is the TPA coefficient ($= 5 \times 10^{-10}$ cm/W) [3], λ is the pump wavelength, $\tau_{\rm eff}$ is the effective carrier lifetime, and $\rm E_p$ is the photon energy.

The effective carrier lifetime depends on the recombination lifetime ($\tau_{\rm r}$) of the carriers at the Si-SiO_2 interface and the diffusion time ($\tau_{\rm tr}$) of the carriers out of the modal area and can be written as: $1/\tau_{eff} = 1/\tau_r + 1/\tau_{tr}$ [7]. Since carriers must diffuse to the Si/SiO_2 interface for recombination to take place, $\tau_{\rm r}$ is linearly proportional to Si film thickness. Similarly, the transit time, $\tau_{\rm tr}$ is proportional to rib width (see Fig. 1 (b)). Hence reducing the waveguide cross section is beneficial as it reduces the effective life time and thus minimizes TPA-induced free carrier absorption.

The evolution of Stokes (S), anti-Stokes (A) and pump (P) fields can be described by the following coupled mode equations (assuming electric fields $|E_P| > |E_S| > |E_A|$) [8, 9]. Here $|\omega_{\rm P} - \omega_{\rm S}| = |\omega_{\rm A} - \omega_{\rm P}| = \Omega$ is the Raman frequency shift and $\Delta k = 2k_P\text{-}k_S\text{-}k_A$ refers to the wavevector mismatch. The depletion of the Stokes and anti-Stokes signals due to two photon absorption (TPA) are neglected.

$$\frac{dE_P}{dz} = -\frac{(\alpha + \Delta\alpha_{FCA}(z))}{2}E_P - \frac{\beta}{2}|E_P|^2 E_P$$
$$\frac{dE_S}{dz} = -\frac{(\alpha + \Delta\alpha_{FCA}(z))}{2}E_S + \kappa_{SS}E_S + \kappa_{SA}E_A^* \exp(-i\Delta kz) \quad (1)$$

DOI: 10.1587/elex.1.298
Received August 03, 2004
Accepted August 05, 2004
Published September 10, 2004

$$\frac{dE_A^*}{dz} = -\frac{(\alpha + \Delta\alpha_{FCA}(z))}{2} E_A^* + \kappa_{AA} E_A^* + \kappa_{AS} E_S \exp(+i\Delta kz)$$

The coupling coefficients are given as follows:

$$\begin{aligned} \kappa_{SS} &= -i \cdot \left(2R + \frac{iG}{2}\right) |E_P|^2, & \kappa_{SA} &= -i \cdot \left(R + \frac{iG}{2}\right) E_P^2 \\ \kappa_{AA} &= i \cdot \left(2R - \frac{iG}{2}\right)^* |E_P|^2, & \kappa_{AS} &= i \cdot \left(R - \frac{iG}{2}\right)^* E_P^{*2} \end{aligned} \tag{2}$$

where, $G = \frac{-i\chi_R^{(3)}(\Omega)4\pi\omega^2}{c^2 k} = 2.0 \times 10^{-8}\, cm/W$ [3] refers to the Raman gain coefficient and $R = \frac{\chi_{NR}^{(3)} 2\pi\omega^2}{c^2 k} = 1.7 \times 10^{-9}\, cm/W$ [10] is the contribution due to non-linear electronic response. α refers to the linear propagation loss and is assumed to be the same for all waves and $\Delta\alpha_{\mathrm{FCA}}$ refers to the nonlinear absorption loss. Numerical solutions to these equations are presented in the following section.

3 Experimental results

The experimental setup shown in the inset of Fig. 2 consists of a CW pump at 1427.3 nm (TE polarized) and an external cavity diode laser (ECDL) used as the Stokes source at 1542.3 nm (TE polarized). The ECDL is amplified before combining with the pump. At the output end, a band-pass filter is used to extract the converted anti-Stokes signal at 1328.8 nm (TE polarized) before

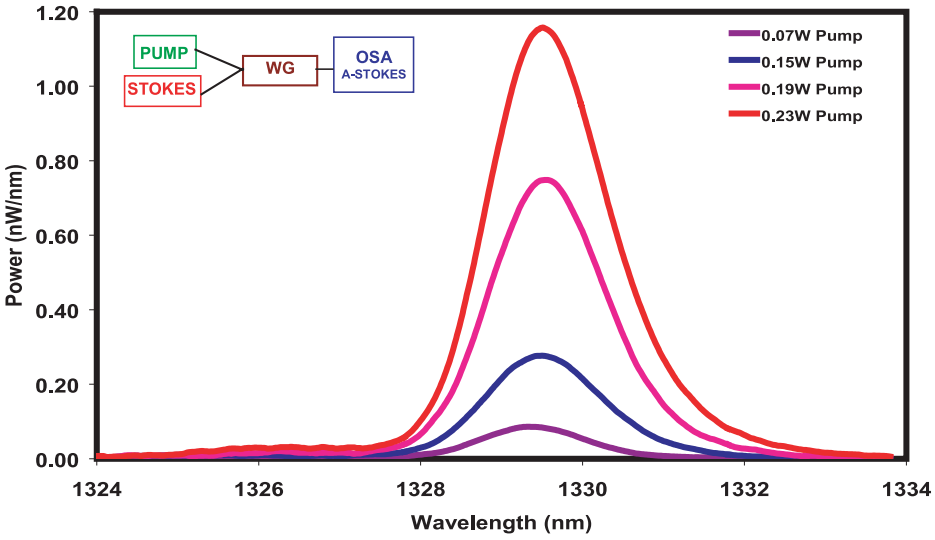

Fig. 2. The experimental setup used for wavelength conversion is shown in the inset. The pump signal (1427.3 nm) and Stokes signal (1542.3 nm) are launched into the waveguide. The propagation loss in these waveguides was ∼2.5 dB/cm. The converted anti-Stokes signal (1328.8 nm) is observed using the Optical spectrum analyzer (OSA). The optical spectrum of converted anti-Stokes signal is shown at various pump powers.

DOI: 10.1587/elex.1.298
Received August 03, 2004
Accepted August 05, 2004
Published September 10, 2004

observing the converted power using an optical spectrum analyzer (OSA). The Silicon-on-Insulator (SOI) rib waveguide used is 2.5 cm long with dimensions as shown in Fig. 1 (b) and a modal area of $\sim$0.54 μm^2. The propagation losses in these waveguides at 1328.8 nm were estimated to be $\sim$2.5 dB/cm. The polarization configuration used in this work is different from our previous report [10, 11]. The reason for this is the different dispersion properties of the submicron modal dimension waveguides as discussed below.

Figure 2 shows the optical spectrum of the converted anti-Stokes signal at 1328.8 nm for an input Stokes power of 1.8 mW. The center wavelength is precisely at the expected shift (520 cm^{-1}) from the pump. There is a clear non-linear growth of the anti-Stokes signal with increase in pump power. A maximum anti-Stokes converted power of 2.3 nW is measured; taking into account the coupling losses, the net conversion efficiency is found to be 1.7x10^{-5}. We note that this is achieved at a lower pump power than our previous reports [10, 11]. The improvement is a manifestation of sub-micron modal dimensions used here.

The experimentally obtained variation of conversion efficiency with pump intensity is shown in Fig. 3 (squares). Theoretical fit to the measured data using the coupled mode equations, with $E_S(0) \neq 0$, $E_A(0) = 0$ shows good agreement for an effective lifetime of 10 ns (solid line) and $15 < |\Delta k| < 120\,\mathrm{cm}^{-1}$. The oscillatory nature of efficiency vs. Δk makes it not possible to extract the exact value of Δk using this method [10]. Also shown is the conversion efficiency when the pump and Stokes fields are orthogonally polarized (triangles). In this case, birefringence contributes to phase mismatch and conversion is found to be less efficient.

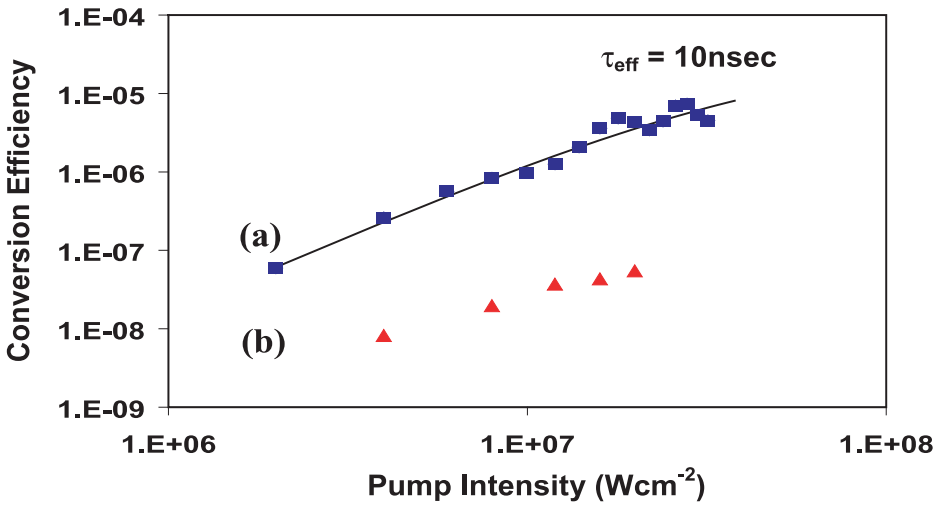

Fig. 3. Experimental plot of conversion efficiency vs. pump intensity: (a) both pump and signal are TE polarized (no birefringence). Theoretical fit shows good agreement for effective lifetimes τ_{eff} of 10 nsec. (b) pump and signal are TE and TM polarized respectively (with birefringence).

DOI: 10.1587/elex.1.298
Received August 03, 2004
Accepted August 05, 2004
Published September 10, 2004

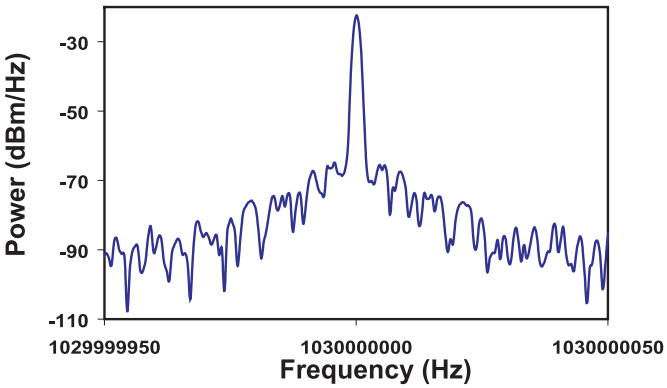

Fig. 4. Conversion of analog RF signal (centered at 1.03 GHz) from Stokes to anti-Stokes. Electrical SNR of 47 dBe was obtained over a bandwidth of 100 Hz.

Figure 4 shows the conversion of a 1.03 GHz electrical signal from Stokes to anti-Stokes. The electrical signal was modulated onto the 1542.3 nm carrier and the RF spectrum of the converted 1328.8 nm signal after photodetection and amplification is shown in this figure. A Signal-to-Noise Ratio (SNR) of 47 dBe is obtained over a 100 Hz bandwidth for the converted signal. Further increase in bandwidth and SNR for the conversion requires Δk close to phase matching.

4 Phase matching in submicron waveguides

Efficient wavelength conversion in Silicon waveguides using the Raman susceptibility requires phase matching between the Stokes, anti-Stokes and pump waves. The phase matching condition is an important part of waveguide design since dispersion, and hence phase mismatch, depend on waveguide dimensions.

The main contributions to phase mismatch are material, waveguide dispersion of the guiding silicon rib structure and birefringence. To achieve phase matching, material dispersion has to be compensated by the combined contributions of waveguide dispersion and birefringence [9]. The TPA induced free-carriers also result in change in refractive index and can alter the phase matching condition. However, this effect is negligible at pump powers used in this work.

In waveguides with relatively large modal area ($\sim$5 μm^2) the contribution of waveguide dispersion is insignificant and birefringence is the only viable means for phase matching [9, 11]. However, in submicron modal area waveguides, such as the ones used in this work, birefringence increases dramatically to the extent that it over-compensates the material dispersion [12]. Fortunately, waveguide dispersion also increases sufficiently [13] that it can provide efficient conversion. This is verified in the experimental results of Fig. 3.

DOI: 10.1587/elex.1.298
Received August 03, 2004
Accepted August 05, 2004
Published September 10, 2004

5 Conclusions

We have demonstrated wavelength conversion in silicon waveguides with submicron modal area. The effects of two photon absorption and free carrier losses on the conversion process have also been analyzed. We find that reducing the rib waveguide dimensions offers two-fold advantage in increasing the conversion efficiency and reducing the free carrier losses. We have measured a conversion efficiency of 1.7×10^{-5}, a value that is limited primarily by phase mismatch. Dispersion engineering by proper rib-structure design would enable phase matching and help in achieving high efficiency wavelength conversion.

Acknowledgments

This work was supported by the MTO office of the Defense Advance Research Project Agency (DARPA). The authors would like to thank Dr. Jagdeep Shah for his support.

DOI: 10.1587/elex.1.298
Received August 03, 2004
Accepted August 05, 2004
Published September 10, 2004